Reproductive Biology and Endocrinology

RESEARCH

Open Access

Broadening the *ARMC2* mutational phenotype: linking multiple morphological abnormalities of the Flagella to Pulmonary Manifestations in Primary Ciliary Dyskinesia

Baoyan Wu[1†], Wenhao Zhang[7†], Hui Yu[1†], Lewen Ruan[1†], Kai Wang[1†], Meng Gu[1], Hao Geng[1,4,5], Jiajun Fang[6], Chuan Xu[1,4,5], Yuying Sheng[1], Qing Tan[1,8], Qunshan Shen[1,8], Zongliu Duan[1,4,5], Huan Wu[1,4,5], Rong Hua[1,4,5], Rui Guo[1,4,5], Zhaolian Wei[1,4,5], Ping Zhou[1,4,5], Yuping Xu[1,4,5], Yunxia Cao[1,2,3], Xiaojin He[9], Kuokuo Li[1,2,3*], Mingrong Lv[1,2,3*] and Dongdong Tang[1,2,3*]

Abstract

Background Severe asthenoteratozoospermia, a prevalent cause of male infertility, has increasingly been associated with *ARMC2* variants that cause Multiple Morphological Abnormalities of the Sperm Flagella (MMAF). Although *ARMC2* is also expressed in other ciliary structures, no studies have yet reported a link between *ARMC2* gene variants and other symptoms of Primary Ciliary Dyskinesia (PCD).

Methods Here, we performed whole-exome sequencing (WES) on Chinese subjects with MMAF to identify potential genetic variants. Sanger sequencing was used to validate the candidate variants. Sperm morphology was assessed using modified hematoxylin and eosin (H&E) staining, and transmission electron microscopy (TEM) was performed to observe the ultrastructural defects of the sperm flagella. Western blot analysis and immunofluorescence (IF) of spermatozoa were performed to evaluate variations in structural protein. Additionally, intracytoplasmic sperm injection (ICSI) was applied for assisted fertilization.

Results We identified two compound heterozygous *ARMC2* variants and one homozygous variant (P1: c.1030_1042del, p.T344fs/c.1331G > A, p.R444H; P2:c.1264C > T, p.R422X) in two unrelated individuals. Notably, in addition to MMAF, individual P2 exhibited classic symptoms of PCD in the lungs, including recurrent airway infections, bronchitis, and rhinosinusitis. Morphological and ultrastructural analyses of the spermatozoa obtained from the two individuals revealed dramatic disorganization in axonemal and peri-axonemal structures, as well as the absence of the axonemal central pair complex (CPC). Immunoblotting and immunofluorescence assays revealed the reduced

[†]Baoyan Wu, Wenhao Zhang, Hui Yu, Lewen Ruan and Kai Wang contributed equally to this work.

*Correspondence:
Kuokuo Li
likuokuo_bio@163.com
Mingrong Lv
lvmingrong2016@163.com
Dongdong Tang
tangdongdong@ahmu.edu.cn
Full list of author information is available at the end of the article

expression of ARMC2 and the abnormality of various axonal structural proteins. Further assisted reproduction outcomes showed that one of the individuals conceived successfully after Intracytoplasmic Sperm Injection (ICSI).

Conclusions Overall, this study significantly expanded the mutational phenotype of *ARMC2*, marking the first discovery of PCD-related pulmonary phenotypes outside of the reproductive system. This work establishes the association between *ARMC2* and typical PCD and lays the groundwork for further investigation into the molecular mechanisms of *ARMC2* in both flagellogenesis and ciliogenesis.

Keywords Male infertility, MMAF, PCD, Flagellum, Cilla, *ARMC2*

Background

Infertility is a concerning problem, affecting about 15% of couples of reproductive age worldwide [1], in which male factors account for about half of all cases of infertility [2]. Male infertility is a highly inherited condition and is usually classified into oligozoospermia, asthenozoospermia, teratozoospermia, and even azoospermia.

Male infertility can be attributed to a variety of factors, including disorders of the genitourinary system, environmental influences, and genetic components. Recently, the role of monogenic variants in male infertility has garnered increasing attention. It is believed that more than 4,000 genes are involved in the process of spermatogenesis [3]. Any defects in these pathogenic genes can hinder sperm production and result in male infertility. Recently, high-throughput sequencing technology has enabled researchers to identify an increasing number of genes necessary for sperm production, significantly advancing our understanding of the genetic basis of various forms of male infertility.

MMAF is a rare but serious subtype of asthenoteratozoospermia, characterized by multiple abnormalities on sperm flagella with a combination of short, absent, coiled, bent, and/or irregular-caliber flagella [4]. To date, genetic variants have been identified in more than 50 genes associated with MMAF, including *AK7* (MIM: 615,364), *AKAP4* (MIM: 300,185), *ARMC2* (MIM: 618,424), *CFAP43* (MIM: 617,558), *CFAP44* (MIM: 617,559), *CFAP65* (MIM: 614,270), *CFAP69* (MIM: 617,949), *DNAH1* (MIM: 603,332), *FSIP2* (MIM: 618,153), *QRICH2* (MIM: 618,304), *SPEF2* (MIM: 610,172), *TTC21A* (MIM: 611,430), and *WDR66* (also known as *CFAP251*, MIM: 618,146), *DRC1*(MIM:615,288) [5–12], et al. At present, the identified variants could account for about 60.0%−75.0% of infertile men diagnosed with MMAF, while the remaining cases (25.0%−40.0% of MMAF patients) have unknown genetic factors. As sperm flagella and motile cilia share similar "9 + 2" axonemal structures, malfunction of the axoneme in these organelles may lead to other ciliary abnormalities, causing phenotypes beyond the reproductive system, such as pulmonary phenotypes, associated with primary ciliary dyskinesia (PCD; MIM: 244,400) [13]. So far, approximately 40 disease-causing genes accounting for ~ 70% of PCD have been implicated in humans [14].

ARMC2 (MIM: 618,424) is located on chromosome 6 and contains 18 exons, encoding an armadillo protein with 867 amino acids, composed of 12 armadillo repeats (ARM-repeat) flanked by unique C-terminal and N-terminal domains (NCBI: NP_115507.4; UniProtKB: Q8NEN0), which is specifically expressed in human testes and spermatozoa. Coutton C et al. first established the pivotal role of *ARMC2* in MMAF using whole-exome sequencing (WES) in a cohort comprising 168 individuals with infertility in 2019 [15]. Although *ARMC2* has been observed to be abundantly expressed in epithelial cells with cilia and sperm flagella, initial findings indicated that *ARMC2* defects were specific to male infertility. To date, no studies have confirmed that biallelic variants in *ARMC2* lead to ciliary defects in other systems. However, it is noteworthy that genome-wide interaction studies have associated *ARMC2* variants with diminished pulmonary function [16, 17], highlighting their potentially extensive involvement in ciliary biology that extends beyond their influence on fertility.

In this study, we have identified biallelic variants in the *ARMC2* gene in two unrelated patients with MMAF. Notably, one patient exhibited additional classical PCD-related pulmonary symptoms, including recurrent airway infections, bronchitis, and rhinosinusitis, in addition to MMAF. Further analysis revealed impaired flagellar assembly in *ARMC2* mutant individuals. Immunoblotting and immunofluorescence assays of the *ARMC2* variant also resulted in significant reductions in ARMC2 protein levels and led to the loss of function of many axonemal structural proteins. Our findings expanded the genetic spectrum of the *ARMC2* gene and provided further understanding of the links between *ARMC2* gene variants and PCD.

Material and methods

Study participants

Subjects diagnosed with MMAF from the First Affiliated Hospital of Anhui Medical University (Hefei, China) were included in this study. The diagnosis and evaluation of subjects were conducted in strict accordance with the

guidelines outlined in the World Health Organization (WHO) Laboratory Manual for the Examination and Processing of Human Semen. Both participants had a normal 46, XY karyotype and no Y chromosome microdeletions. Potential causes of infertility, such as iatrogenic injury, reproductive tract infections, testicular inflammation, and drug exposure, were carefully excluded. Physical examinations revealed normal findings, verifying typical parameters for height, weight, hair distribution, mental state, testis size, and external genital organs.

Ethical approval for the genetic study was granted by the corresponding ethics committees of the First Affiliated Hospital of Anhui Medical University (PJ2023-04–19). Both individuals provided written informed consent prior to participation in the study.

Semen parameters and sperm morphological analysis

According to the guidelines of the World Health Organization (WHO, 2010) [18], subjects collected semen samples by masturbation after 2–7 days of abstinence. The samples were then analyzed in the source laboratory during routine biological examination. We used hematoxylin and eosin (H&E) staining to evaluate sperm morphology. For each subject, we examined at least 200 spermatozoa to evaluate the percentage of sperm with abnormal morphology.

Whole-Exome Sequencing (WES) and bioinformatic analysis

Genomic DNA was extracted from peripheral blood samples of asthenoteratozoospermic individuals for Whole-Exome Sequencing (WES). DNA was sheared into fragments, enriched using a Sure Select XT Human All Exon Kit, and sequenced using an Illumina HiSeq X-TEN platform. Sequenced reads were mapped to the human reference GRCh38/hg19 genome using Burrows-Wheeler Aligner (BWA) software [19]. Annotation of the variants was performed using ANNOVAR [20], incorporating data from several public databases, including the 1000 Genomes Project and gnomAD. Potentially deleterious variants were evaluated using SIFT, MutationTaster, PolyPhen-2, and the Combined Annotation-Dependent Depletion (CADD) score. Common variants with an allele frequency of > 0.05 were excluded. Our focus was on loss-of-function variants, including splicing variants (< 2 bp), stop gains, stop losses, frameshift indels and deleterious missense variants. Missense variants predicted to be deleterious by at least three of the four software tools- SIFT, PolyPhen-2, MutationTaster, and CADD (score > 20)- were defined as deleterious. We determined conservation among species by performing an alignment of the amino acid sequences of ARMC2 proteins whose data were obtained from the GenBank database. *ARMC2* variants identified through WES were further validated by Sanger sequencing, with the primers used for validation provided in Table S1.

Transmission electron microscopy (TEM)

The patient's sperm and the control group's sperm were washed three times with 1 × phosphate-buffered saline (PBS) at 2500 rpm at 25 °C, and then fixed with 2.5% glutaraldehyde (pH 6.9) for more than 2 h at 4 °C. Immobilized sperm were fixed with 1% osmium tetroxide for 2 h at 4 °C, stained with 2% uranium acetate for 2 h, and dehydrated in a graded series of ethanol (50%, 70%, 90% and 100%) and 100% acetone. Then, the fixed spermatozoa were embedded in EPON 812 epoxy resin. Finally, it was cut into 100-nm sections by using an EM UC7 microtome (Leica, Wezlar, Germany), stained with lead citrate, and observed under a TEM (Thermo Fisher Scientific, Waltham, MA, USA) by using Talos L120C G2.

Western blot (WB) analysis

Protein was isolated from patients' sperm samples and control sperm samples by RIPA lysis buffer (Beyotime Biotechnology) for western blot analysis. Lysates were separated on 10% polyacrylamide gel by sodium dodecyl sulfate–polyacrylamide gel electrophoresis and transferred to PDVF membrane. To prevent non-specific binding to the membrane, the blot was blocked with 5% non-fat milk in Tris-buffered saline containing 0.1% Tween-20 at 25 °C for 1 h. The primary antibody diluted with TBST was then incubated overnight at 4 °C by shaking. Rabbit polyclonal anti-TOMM20 (1:1000), rabbit polyclonal anti-SPAG6 (1:1000), rabbit polyclonal anti-IFT88 (1:1000), rabbit polyclonal anti-ARMC2 (1:1000), and mouse polyclonal anti-β-Actin were used. Subsequently, these blots were washed in TBST and incubated at 25 °C for 1 h with 1:5000 dilutions of HRP-conjugated secondary antibody. Enhanced chemiluminescence (Biosharp, BL520A) was used to visualize the target protein, and β-Actin was used as a loading control.

Immunofluorescence analysis

Immunofluorescence analysis was performed with sperm cells from healthy controls and patients carrying *ARMC2* variants. Sperm cells were washed in phosphate-buffered saline (PBS), fixed in 4% paraformaldehyde for 30 min at room temperature, and coated on a glass slide precoated with 0.1% poly-L-lysozyme (Thermo Scientific). Then, the slides were washed in PBS, blocked in 10% donkey serum, and incubated overnight at 4 °C with the following main antibodies: rabbit polyclonal anti-ARMC2 (1:100), rabbit polyclonal anti-TOMM20 (1:200), rabbit polyclonal anti-SPAG6 (Sigma-Aldrich, HPA038440, 1:200), rabbit polyclonal anti-IFT88 (Proteintech, 13,967–1-AP, 1:200),

as well as mouse monoclonal anti-acetylated α-tubulin (Sigma-Aldrich, T6793, 1:200). After washing with PBS, slides were incubated for 1 h at 37 °C with highly cross-adsorbed secondary antibodies: anti-mouse Alexa Fluor 488 (Yeasen Biotechnology, USA, 34106ES60, 1:500) and anti-rabbit Alexa Fluor 594 antibodies (Jackson ImmunoResearch, USA, 111–585–003, 1:500). DNA was stained using Hoechst 33,342 (Thermo Fisher Scientific, USA, 62, 249, 1:1000). The images were captured with the LSM 800 confocal microscope (Carl Zeiss AG).

Intracytoplasmic sperm injection procedure

Among the individuals with the *ARMC2* variant, one patient received ICSI treatment. The patient's wife underwent a long protocol to induce ovulation. To enrich sperm vitality, semen samples were centrifuged with a discontinuous density gradient. After egg retrieval, mature oocytes and motile sperm were selected for ICSI. All embryos formed after standard embryo culture are preserved by vitrification for the next freeze–thaw cycle. Two months later, one or two viable blastocysts were thawed and transferred to the uterus of the female partner. Serum β-HCG level was measured on the 14th day after embryo transfer to confirm biochemical pregnancy, and clinical pregnancy was confirmed by B-ultrasound on the 30th day after embryo transfer.

Results

Bi-allelic *ARMC2* variants were identified in two unrelated individuals with MMAF

In this study, we identified two compound heterozygous *ARMC2* variants and one homozygous variant (P1: c.1030_1042del, p.T344fs/c.1331G > A, p.R444H; P2:c.1264C > T, p.R422X) in two unrelated individuals. Sanger sequencing confirmed that their parents were heterozygous carriers in the two unrelated families, which was consistent with an autosomal recessive mode of inheritance (Fig. 1A). The prevalence analysis from the 1000 Genomes and gnomAD databases revealed that these variants were either at low allele frequencies or unavailable in the general population, suggesting their rarity (Table S2). In addition, the frameshift and nonsense variants (M1, M3) identified in this study were assumed to induce premature termination codons and truncated proteins. The remaining missense variant, M2, caused the substitution of arginine (R) with histidine (H) and was highly conserved among species (Fig. 1B). It was also predicted to be deleterious by bioinformatic tools such as SIFT, PolyPhen-2, Mutation Taster, and CADD (Table S2).

Clinical features of two subjects with bi-allelic *ARMC2* variants

Clinical examination revealed normal male testicular size, external genitalia, hormone levels, and secondary sexual characteristics. Chromosomal karyotype analysis showed no abnormalities. Semen analysis and sperm morphology assessment indicated asthenoteratozoospermia and typical MMAF. The P1 individual exhibited no other symptoms associated with PCD; however, the P2 individual exhibited not only typical MMAF but also characteristic PCD-related pulmonary phenotypes, including recurrent airway infections, bronchitis, and rhinosinusitis (Table 1). A chest CT scan of P2 showed bilateral lower lung bronchiectasis and typical imaging manifestations like signet ring sign (Fig. 2C). It was shown that semen volume and sperm concentration were within normal ranges in both individuals carrying bi-allelic *ARMC2* variants, while a significant reduction was observed in sperm motility and progressive motility. Morphological analysis of the patients' sperm revealed a typical phenotype of MMAF, characterized by absent, coiled, short, bent, and irregular caliber flagella. Among these abnormalities, the most frequently observed defects were short and curly flagella in the sperm of both patients (Table 1 and Fig. 2A).

To investigate the sperm flagellar ultrastructure of individuals harboring bi-allelic *ARMC2* variants, we performed TEM analyses of spermatozoa obtained from two patients and healthy control individuals. More than 50 flagella cross-sections were randomly observed under TEM to evaluate the microtubule assembly in sperm flagella. In the control sperm, typical "9 + 2" microtubule structures were observed, consisting of a central pair of microtubules surrounded by nine peripheral microtubule doublets. These doublets were supported by nine radial spoke complexes and were encased by outer dense fibers

(See figure on next page.)

Fig. 1 Identification of Bi-allelic variants in *ARMC2*. **A** Pedigrees of two families carrying *ARMC2* variants. All the affected individuals have bi-allelic variants with a recessive inheritance mode. P1 carries compound heterozygous variants of *ARMC2* derived from his parental heterozygous carriers. P2 has homozygous variants in *ARMC2*. Sanger sequencing results are shown below the pedigrees. The deleted region in the Sanger sequencing chromatogram for M1 is highlighted with a red box, and the position of each variant for M2 and M3 is indicated by a red arrow. **B** Schematic representation of the functional domains of ARMC2 and the locations of *ARMC2* variants identified in this study. Arrows (red) and dotted lines (blue, red and black) show the positions of novel *ARMC2* variants identified in the present study. Sequence alignments show that the amino acid affected by the M2 mutation is highly conserved across different species. The blue boxes indicate 12 ARM repeat domains as described by the Uniprot server. Abbreviations: M1, mutation 1; M2, mutation 2; M3, mutation 3; WT, wild type

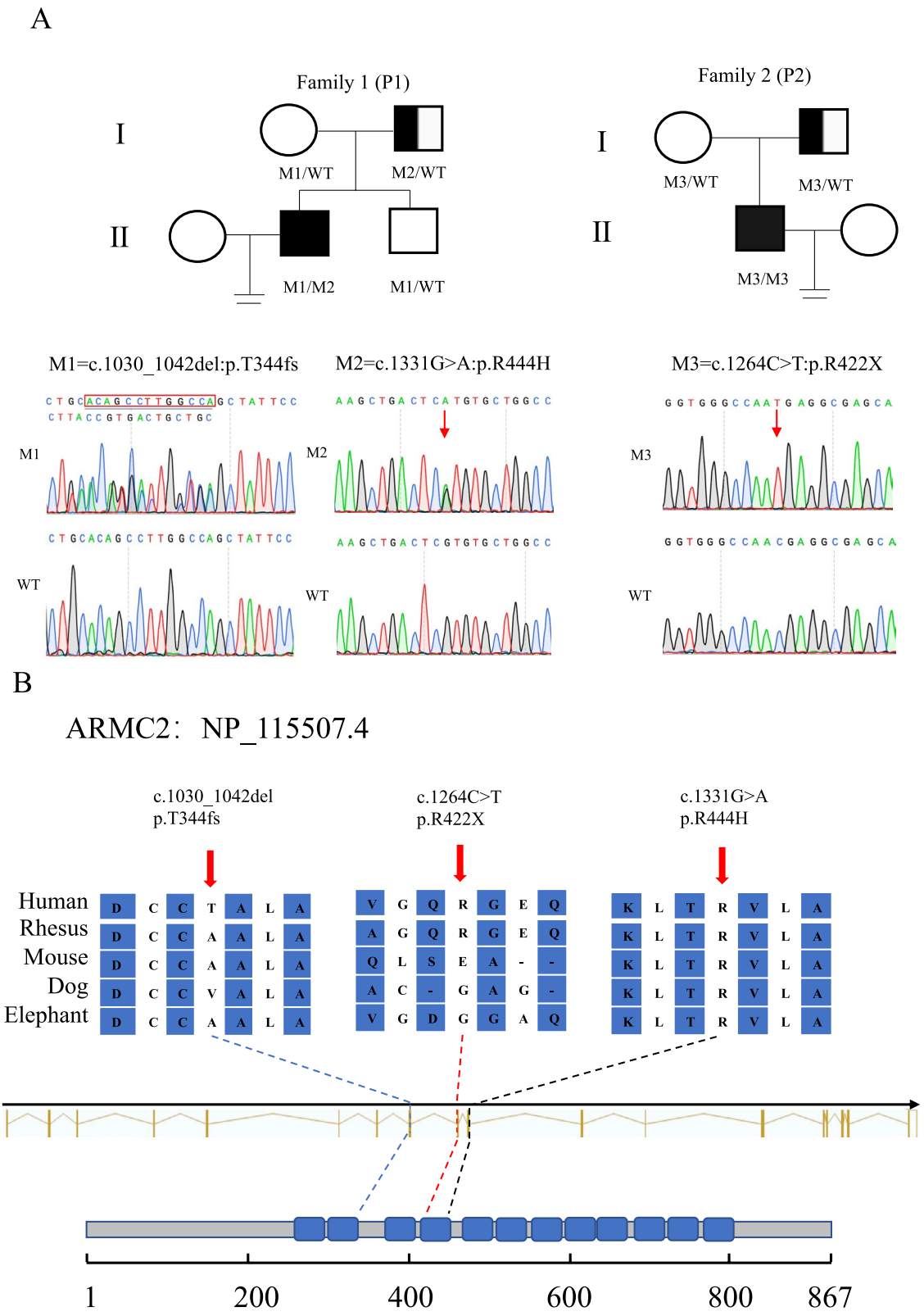

Fig. 1 (See legend on previous page.)

Table 1 Clinical features in Men Harboring ARMC2 Variants

Subject	P1	P2	Reference Limits
Semen Parameter			
Semen volume (ml)	1.5	3.2	> 1.5
Semen pH	7.5	7.5	
Semen concentration (10^6/mL)	19.2	44.5	> 15.0
Motility (%)	41.5	0	> 40.0
Progressive motility (%)	23.2	0	> 32.0
Sperm Morphology			
Normal tail (%)	6.4 (13/202)	5.9 (12/202)	> 23.0
Absent flagella (%)	23.3 (47/202)	37.1 (75/202)	< 5.0
Short flagella (%)	27.7 (56/202)	42.1 (85/202)	< 1.0
Coiled flagella (%)	42.6 (86/202)	14.9 (30/202)	< 17.0
DNA Fragmentation Index (DFI)%	13.4	29.9	< 15
Phenotypic features			
Airway Disease			
Recurrent airway infections	NO	Yes	
Bronchiectasis	NO	Yes	
Rhinosinusitis	NO	Yes	
Otitis media	NO	Yes	
Situs inversus	NO	NO	
Infertility	Yes	Yes	

(ODF). However, the sperm flagella of the two individuals harboring biallelic *ARMC2* variants mainly presented a dramatic disorganization in axonemal or other periaxonemal structures. The main defect observed in sperm flagella was the lack of a central pair of microtubules, resulting in an abnormal "9 + 0" configuration. In addition, the peripheral microtubule doublets, outer dense fibers, and mitochondrial sheath were also translocated and disordered (Fig. 2B).

Sperm flagellar component defects in patients with bi-allelic *ARMC2* variants

To investigate the impact of *ARMC2* biallelic variants on sperm flagellar composition, we first examined the expression and localization of ARMC2. WB and immunofluorescence analyses revealed that ARMC2 immunostaining was predominantly localized along the entire length of the flagella, with limited protein signals observed in the acrosomal region and neck of normal sperm. However, in the P2 individual carrying the *ARMC2* homozygous variant, these signals were almost absent (Fig. 3A). Correspondingly, WB analysis demonstrated that ARMC2 was either absent or significantly downregulated in spermatozoa from the P2 individual (Fig. 3B). To comprehensively investigate the effects of biallelic variant in *ARMC2* on the assembly or anchoring of axonemal proteins complexes, WB and immunofluorescence analyses were subsequently performed

(See figure on next page.)

Fig. 2 Sperm Morphology and Ultrastructure Analyses for Men Harboring *ARMC2* Variants**. A** Light microscopy analysis of spermatozoa from the control and men harboring *ARMC2* variants. Most spermatozoa from men harboring *ARMC2* variants have flagella that are short, coiled, or of irregular caliber. The spermatozoa from subjects P1 and P2 are given as examples of typical MMAF phenotypes observed in men harboring *ARMC2* variants. Scale bars: 10 μm. **B** TEM analyses of sperm cells from a fertile control and two men harboring *ARMC2* variants. The control individual shows the typical "9 + 2" microtubule structure, including nine peripheral microtubule doublets paired with nine outer dense fibers and the central pair of microtubules, surrounded by the organized mitochondrial sheath or fibrous sheath. The ultrastructure observed in cross-sections of the flagella in men harboring *ARMC2* variants indicates the misarranged outer dense fibers and disorganization of the peripheral microtubules with a lack of the central pair of microtubules. Scale bars: 500 nm. Abbreviations: MS, mitochondrial sheath (yellow arrows); CP, central pair of microtubules (orange arrows); MD, microtubules doublet (green arrows); ODF, outer dense fiber (blue arrows). **C** In the lung window, P2-I demonstrated bilateral lower lung bronchiectasis with characteristic imaging features, including the signet ring sign (red arrows). In the mediastinal window, P2-II displayed normal anatomical positioning of the liver (blue arrows), spleen (yellow arrows), and stomach (green arrows), with no evidence of situs inversus

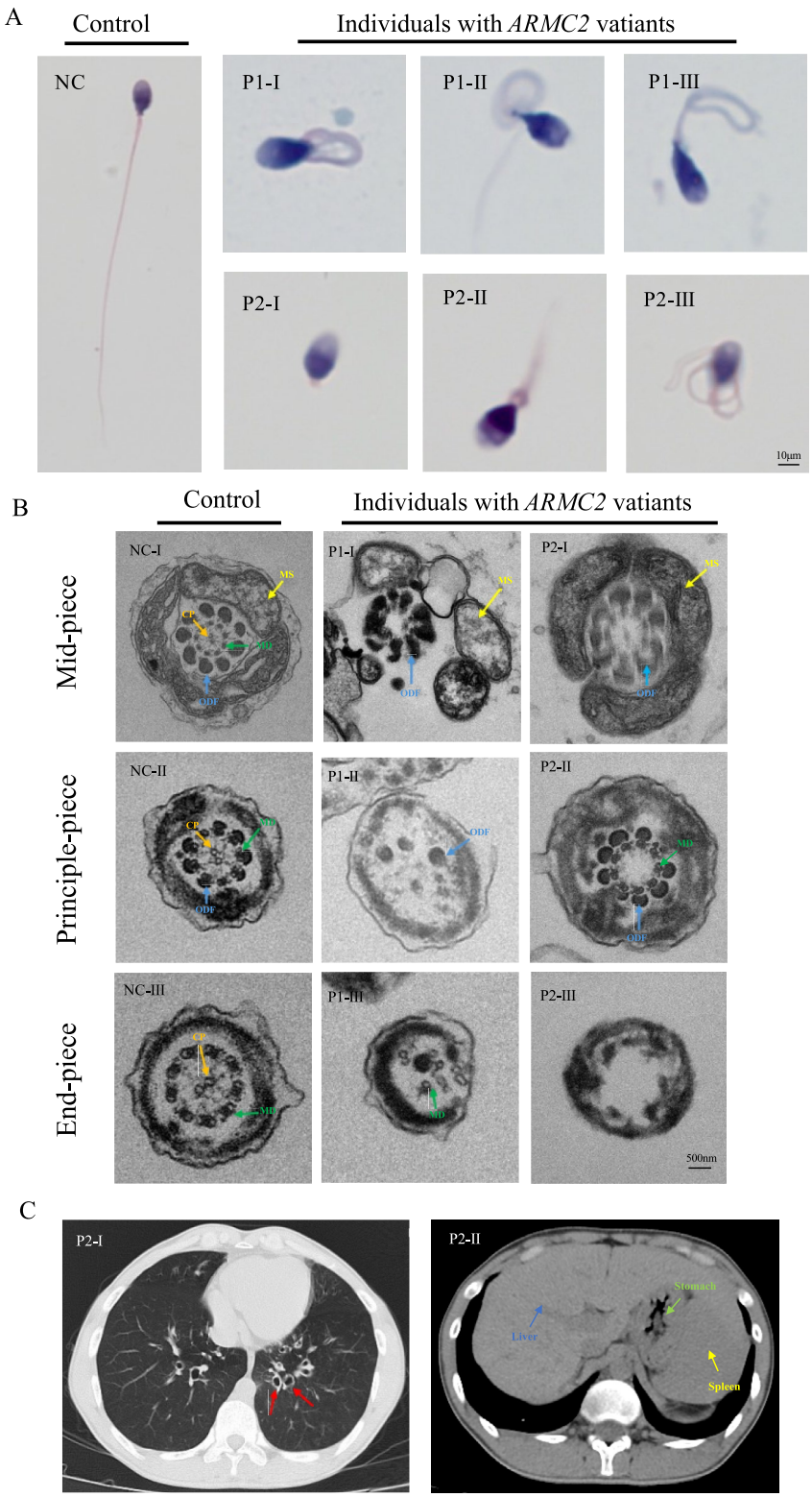

Fig. 2 (See legend on previous page.)

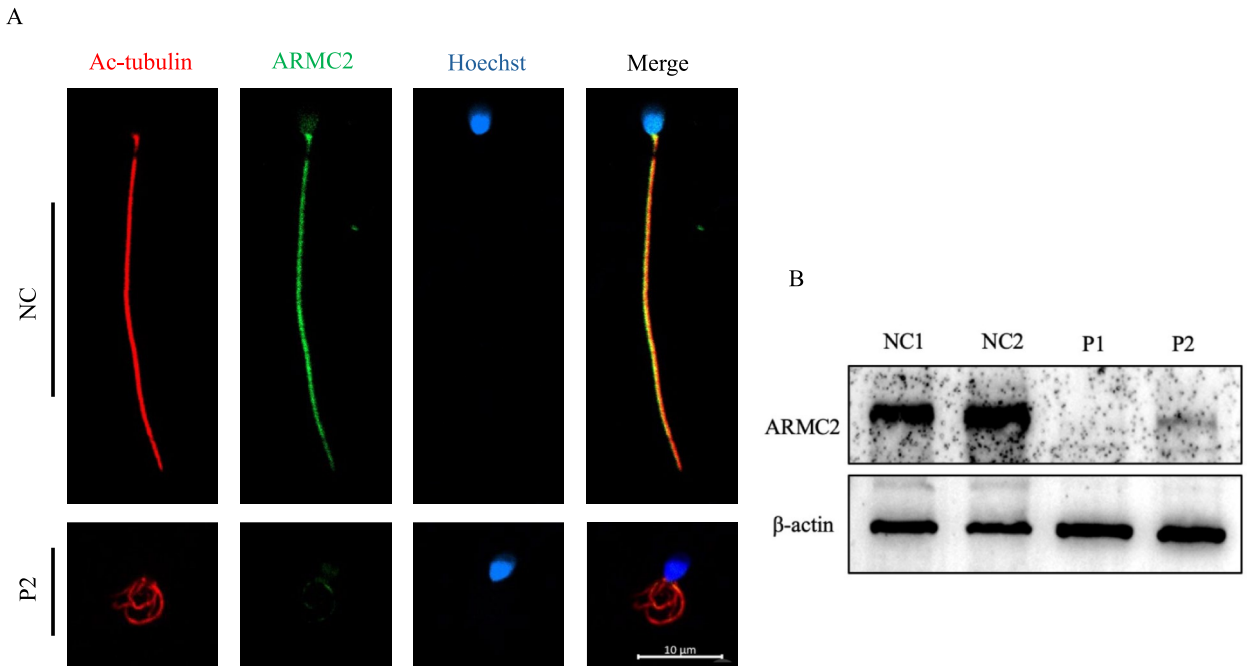

Fig. 3 Expression Analysis and Location of ARMC2 Protein in Sperm Flagella. **A** ARMC2 immunostaining in human spermatozoa from a normal control and men harboring *ARMC2* variants. Sperm cells were stained with anti-ARMC2 (green) and anti-Ac-Tubulin (red) antibodies. DNA was counterstained with Hoechst as a nuclei marker. ARMC2 immunostaining is localized along the entire flagella but is almost absent in the sperm flagella of men harboring *ARMC2* variants. Scale bar: 10 μm. **B** Immunoblotting analysis of ARMC2 protein in sperm lysates from a normal control and men harboring *ARMC2* variants (P1 and P2). WB assays suggested that the level of ARMC2 was reduced significantly in the sperm from men harboring *ARMC2* variants when compared to the level in sperm from a normal control man. β-Actin was used as a loading control

with antibodies targeting proteins located in various axonemal and peri-axonemal structures of the sperm flagella, including SPAG6 (a component of CP complex), TOMM20 (a mitochondrial outer membrane protein) and IFT-88 (a component of IFT-B subcomplex). WB assays performed on spermatozoa from subjects P1 and P2 revealed a dramatic reduction or complete absence of SPAG6 signals. Moreover, immunostaining assays performed specifically on spermatozoa from subject P2 also showed a complete absence of SPAG6 signals. In addition, WB assays revealed that the expression levels of TOMM20 and IFT-88 were significantly reduced in P1, whereas the reduction was not evident in P2. Immunofluorescence assays also showed similar results (Fig. 4A-D). This finding implied that *ARMC2* deficiency primarily led to a significant reduction in SPAG6 levels, thereby impairing the assembly of the central pair complex (CPC).

Favorable outcomes via ICSI in subjects with *ARMC2* variants

The partners of the two individuals harboring bi-allelic *ARMC2* variants had been unable to conceive spontaneously without contraception for over two years. Current studies have predominantly indicated that ICSI is an effective treatment for patients with MMAF. The partner of P2 had an irregular menstrual cycle. Seven oocytes were retrieved, all of which were at the metaphase II (MII) stage and subsequently microinjected. Successful fertilization occurred in seven oocytes, which then cleaved. On the first day post-fertilization, four embryos showed two pronuclei (2PN), and three showed no pronuclei (0PN). By the fifth and sixth days, six blastocysts were developed and subsequently cryopreserved. Following thawing and embryo transfer, a positive urinary hCG test was observed 14 days post-transfer. At 30 days post-transfer, a singleton intrauterine pregnancy was confirmed via ultrasound. Ultimately, a healthy baby boy was successfully delivered (refer to Table 2 for detailed data). Although we lack information on the assisted reproductive cycle of P1, the successful outcome in P2 suggested that ICSI could be a viable clinical treatment option for patients with *ARMC2* variants.

Discussion

In this study, we identified bi-allelic variants of *ARMC2* in two unrelated individuals with MMAF. Moreover, in one of these patients, we found for the first time that bi-allelic variants of *ARMC2* not only lead to MMAF but may also be associated with PCD-related pulmonary

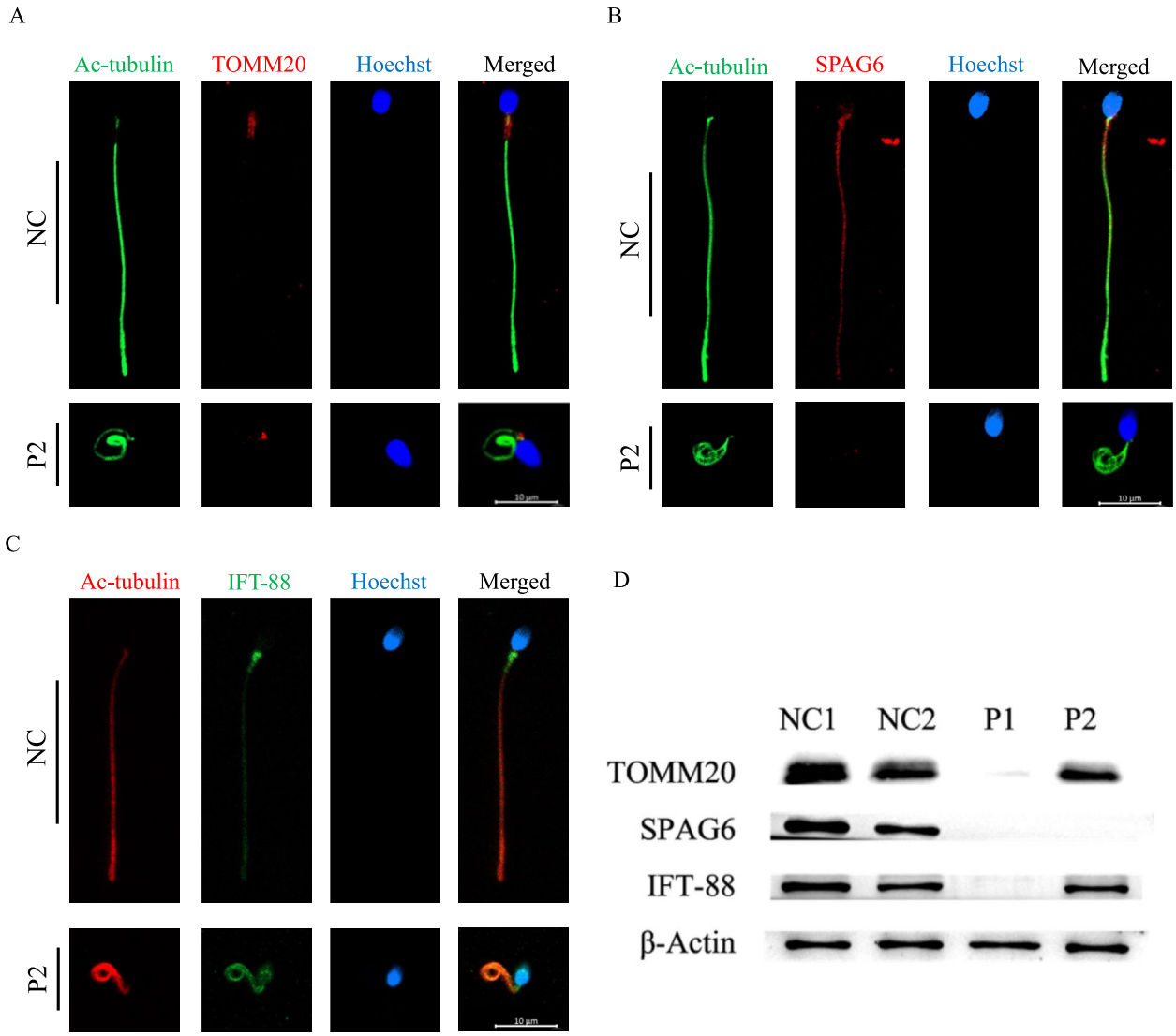

Fig. 4 The localization and levels of flagella-associated proteins in *ARMC2* patients and controls. **(A-C)** Immunofluorescence assays of flagella-associated proteins, including TOMM20 (mitochondrial outer membrane protein), SPAG6 (a component of the CP complex), and IFT 88 (a component of IFT-B subcomplex) in *ARMC2* patients and controls. Anti-TOMM20 (red in A) localized at mitochondrial sheath, Anti-SPAG6 (red in B), Anti-IFT-88 (green in C) were normally localized along the sperm flagella in the control sperm. A complete absence of SPAG6 signals was observed in P2. Anti-Ac-Tubulin (green in A and B, red in C) marked the sperm flagella, and Hoechst (blue) marked the nucleus of spermatozoa. Scale bar: 10 μm. **(D)** WB assays analyzed the expression levels of TOMM20, SPAG6, and IFI-88 in sperm obtained from *ARMC2* individuals and normal controls. The results of WB assays were consistent with those of immunofluorescence assays described above. β-Actin was used as a loading control

phenotypes. This expands the phenotypic spectrum of *ARMC2* variants and suggests that *ARMC2* is a new candidate gene for PCD.

ARMC2 encodes a protein containing several armadillo (ARM) repeats [21], which are involved in a wide range of cellular functions, including cytoskeleton regulation, intracellular signal transduction, and protein degradation or folding [22]. Previous studies had shown that ARM-containing domain may have been a key domain in a protein family related to the structure and function of flagella/cilla. Many members of the ARMC protein family were closely related to spermatogenesis or ciliogenesis. For example, ARMC9 played an important role in ciliary development and was related to Joubert syndrome, a hereditary disease [23]. ARMCX4 was found to be involved in the differentiation of spermatogonial stem cells during spermatogenesis [24]. More interestingly, as a sperm mitochondrial outer membrane-related protein, ARMC12 interacted with mitochondrial proteins, such as VDAC2 and VDAC3, to participate in the formation

Table 2 The clinical outcomes of *ARMC2* mutated subject ICSI

Subject	P2
Mean male age (years)	25
Mean female age (years)	25
No. of ICSI cycles	2
No. of oocytes retrieved	7
No. of oocytes injected	7
Fertilization rate (%)	100(7/7)
Cleavage rate (%)	100(7/7)
8-Cell formation rate (%)	85.7(6/7)
Blastocyst formation rate (%)	100(7/7)
High quality blastocyst rate (%)	42.9(3/7)
Number of embryos transferred per cycle	1
Implantation rate (%)	100(1/1)
Clinical pregnancy rate per transfer cycle (%)	100(1/1)
Miscarriage rate (%)	0

of the sperm mitochondrial outer membrane and mitochondrial sheath [25]. Another protein related to the ARM-domain, CFAP69, was closely associated with the formation of central microtubules during sperm flagella development [8]. In our study, all MMAF-related variants in *ARMC2* were located in the ARM domain, which may lead to damage in the ARM domain of the ARMC2 protein. IF and WB analyses also showed that the expression of ARMC2 in the sperm of subjects harboring *ARMC2* variants was significantly reduced compared with normal controls. Therefore, it is speculated that the defect in the ARM domain of the ARMC2 protein may be an important factor contributing to the MMAF phenotype.

Several genes causing MMAF have been identified, and some of these also result in other PCD-related phenotypes. For example, mutations in the *DNAH1* gene, which encodes an inner arm heavy chain dynein, have been associated with MMAF, exhibiting no apparent PCD phenotypes. However, defects in *DNAH1* have also been documented to elicit a PCD phenotype in a female of Arabian descent, as well as a PCD phenotype accompanied by male infertility in mice [26, 27]. Guo et al. reported a *BRWD1* variant associated with MMAF and PCD-like symptoms in humans [28]. Additionally, mutations in *CFAP47*, a gene previously implicated in MMAF, also play a role in the respiratory defects observed in PCD patients [29]. This suggests that some individuals diagnosed with MMAF may exhibit a mild or atypical PCD phenotype. As for *ARMC2*, it is known as a gene linked to MMAF and is implicated in diminished lung function. However, there have been no previous reports of other typical PCD-related symptoms associated with *ARMC2* variants. We have identified the initial case of a patient harboring a homozygous *ARMC2* variant presenting with MMAF and typical PCD-related lung manifestations. Variants in the *ARMC2* gene are hypothesized to trigger PCD via multiple mechanisms. Firstly, such variants might induce aberrations in the axonemal structure, compromising the functionality of dynein arms and nexin links that are crucial for the synchronized movement of cilia, thereby leading to the hallmark ciliary motility deficits in PCD. Secondly, given the potential role of *ARMC2* in ciliary assembly or maintenance, variants could result in anomalies of ciliogenesis or ciliary structural integrity, further contributing to the complex pathophysiology of PCD. Future studies should include comprehensive functional analyses of *ARMC2* to determine its role in cilia biology. Additionally, genetic screening in larger cohorts of PCD patients, coupled with advanced imaging techniques to assess ciliary structure and motility, will be instrumental in establishing a definitive link between *ARMC2* variants and PCD.

Assisted reproductive technology (ART), such as IVF (In vitro fertilization) and ICSI, has become an important tool in treating infertile couples [30]. For MMAF, there is no empirical drug treatment to improve semen parameters; therefore, ICSI may be the only choice for MMAF-affected cases [31]. In previous reports, several variants of *ARMC2* were identified in MMAF patients, and one patient achieved good clinical results after undergoing ICSI-assisted reproductive therapy. In this study, the fertilization rate, pregnancy rate, and delivery rate of the patient's partner were all 100%. Our study further confirmed that patients with bi-allelic variants in the *ARMC2* gene can achieve favorable fertility outcomes after undergoing ICSI, even with PCD.

Although our study provides valuable insights into the association between biallelic *ARMC2* mutations and phenotypes such as MMAF and PCD, several limitations should be noted. First, the small sample size of only two cases limits the generalizability of our conclusions, and larger cohort studies are needed to validate the relationship between biallelic *ARMC2* mutations and these clinical phenotypes. Second, due to the unavailability of appropriate samples, we were unable to conduct immunofluorescence analysis for P1. Third, the lack of imaging scans for P1, along with the absence of nasal nitric oxide (NO) measurements and TEM analysis of respiratory cilia, restricted our ability to comprehensively evaluate the patient's condition. These limitations underscore the need for future studies with larger sample sizes and more thorough phenotypic assessments to confirm and expand upon our findings.

Conclusion

In conclusion, our study further confirmed the association between bi-allelic variants in *ARMC2* and human MMAF. More importantly, we have established, for the first time, a relationship between bi-allelic variants in *ARMC2* and the typical pulmonary phenotype associated with PCD, beyond reproductive phenotypes. Additionally, our results also indicated that male infertility and MMAF resulting from bi-allelic variants in *ARMC2* can be overcome by ICSI, even in the presence of typical PCD. Overall, this research enhanced our understanding of the genetic underpinnings of both flagellar assembly and ciliary function. It offers valuable insights into the genetic causes of male infertility associated with PCD and establishes a foundation for further exploration into the molecular mechanisms of *ARMC2* in flagellogenesis and ciliogenesis.

Abbreviations

MMAF	Multiple Morphological Abnormalities of the Sperm Flagella
PCD	Primary Ciliary Dyskinesia
WES	Whole exome sequencing
H&E	Hematoxylin and eosin
TEM	Transmission electron microscopy
IF	Immunofluorescence
ICSI	Intracytoplasmic sperm injection
CPC	Central pair complex
WHO	World Health Organization
WB	Western blot
ODF	Outer dense fiber
ART	Assisted reproductive technology
IVF	In vitro fertilization

Supplementary Information

The online version contains supplementary material available at https://doi.org/10.1186/s12958-025-01385-0.

Additional file 1.

Additional file 2.

Acknowledgements

We want to thank all the individuals who participated in and supported this research.

Authors' contributions

DT, ML and KL designed the study. BW, WZ, HY, LR, KW collected the samples and data. MG, HG, JF, CX, YS, QT, QS, ZD, HW, RH performed the data analysis. BW, WZ, HY wrote the draft. RG, ZW, PZ, YX, YC and XH revised the draft. All authors have read and approved the final manuscript.

Funding

This work was supported by the National Natural Science Foundation of China (Grant no: 82071705, 82271639 and 82101681), University Outstanding Youth Program of Anhui Provincial Education Department (2022AH030113).

Data availability

No datasets were generated or analysed during the current study.

Declarations

Ethics approval and consent to participate

The local research ethics committee of the First Affiliated Hospital of Anhui Medical University approved this study. Informed consent was obtained from all subjects. All methods were carried out in accordance with relevant guidelines and regulations.

Consent for publication

Not applicable.

Competing interests

The authors declare no competing interests.

Author details

[1]Reproductive Medicine Center, Department of Obstetrics and Gynecology, The First Affiliated Hospital of Anhui Medical University, Hefei 230022, China. [2]NHC Key Laboratory of Study on Abnormal Gametes and Reproductive Tract (Anhui Medical University), Hefei 230032, China. [3]Key Laboratory of Population Health Across Life Cycle (Anhui Medical University), Ministry of Education of the People's Republic of China, Hefei 230032, China. [4]Anhui Province Key Laboratory of Reproductive Health and Genetics, Hefei, Anhui, China. [5]Biopreservation and Artificial Organs, Anhui Provincial Engineering Research Center, Anhui Medical University, Hefei, Anhui, China. [6]The First Clinical Medical College of Anhui Medical University, Hefei 230032, China. [7]Department of Clinical Medical, First Clinical Medical College, Anhui Medical University, Hefei 230032, China. [8]Anhui Provincial Human Sperm Bank First Affiliated Hospital of Anhui Medical University, Hefei, China. [9]Reproductive Medicine Center, Department of Obstetrics and Gynecology, Shanghai General Hospital, Shanghai Jiao Tong University School of Medicine, Shanghai, China.

Received: 7 August 2024 Accepted: 17 March 2025
Published online: 29 March 2025

References

1. Matzuk MM, Lamb DJ. Genetic dissection of mammalian fertility pathways. Nat Cell Biol. 2002;4(Suppl):s41–9.
2. Vander Borght M, Wyns C. Fertility and infertility: definition and epidemiology. Clin Biochem. 2018;62:2–10.
3. Jan SZ, Vormer TL, Jongejan A, Röling MD, Silber SJ, de Rooij DG, et al. Unraveling transcriptome dynamics in human spermatogenesis. Development. 2017;144(20):3659–73.
4. Ben Khelifa M, Coutton C, Zouari R, Karaouzène T, Rendu J, Bidart M, et al. Mutations in DNAH1, which encodes an inner arm heavy chain dynein, lead to male infertility from multiple morphological abnormalities of the sperm flagella. Am J Hum Genet. 2014;94(1):95–104.
5. Baccetti B, Collodel G, Estenoz M, Manca D, Moretti E, Piomboni P. Gene deletions in an infertile man with sperm fibrous sheath dysplasia. Hum Reprod. 2005;20(10):2790–4.
6. Amiri-Yekta A, Coutton C, Kherraf ZE, Karaouzène T, Le Tanno P, Sanati MH, et al. Whole-exome sequencing of familial cases of multiple morphological abnormalities of the sperm flagella (MMAF) reveals new DNAH1 mutations. Hum Reprod. 2016;31(12):2872–80.
7. Tang S, Wang X, Li W, Yang X, Li Z, Liu W, et al. Biallelic mutations in CFAP43 and CFAP44 cause male infertility with multiple morphological abnormalities of the Sperm Flagella. Am J Hum Genet. 2017;100(6):854–64.
8. Dong FN, Amiri-Yekta A, Martinez G, Saut A, Tek J, Stouvenel L, et al. Absence of CFAP69 causes male infertility due to multiple morphological abnormalities of the flagella in human and mouse. Am J Hum Genet. 2018;102(4):636–48.
9. Kherraf ZE, Amiri-Yekta A, Dacheux D, Karaouzène T, Coutton C, Christou-Kent M, et al. A homozygous ancestral SVA-insertion-mediated deletion in WDR66 induces multiple morphological abnormalities of the sperm flagellum and male infertility. Am J Hum Genet. 2018;103(3):400–12.
10. Auguste Y, Delague V, Desvignes JP, Longepied G, Gnisci A, Besnier P, et al. Loss of calmodulin- and radial-spoke-associated complex protein

CFAP251 leads to immotile spermatozoa lacking mitochondria and infertility in men. Am J Hum Genet. 2018;103(3):413–20.
11. Tebbakh C, Barbotin AL, Martinez G, Boursier A, Wehbe Z, Hammouda A, et al. A recurrent loss-of-function variant in DRC1 causes non-syndromic severe asthenozoospermia with favorable intracytoplasmic sperm injection and pregnancy outcomes. Andrology. 2025; https://doi.org/10.1111/andr.13837.
12. Wang J, Wang W, Shen L, Zheng A, Meng Q, Li H, et al. Clinical detection, diagnosis and treatment of morphological abnormalities of sperm flagella: a review of literature. Front Genet. 2022;13: 1034951.
13. Krausz C, Riera-Escamilla A. Genetics of male infertility. Nat Rev Urol. 2018;15(6):369–84.
14. Fassad MR, Shoemark A, le Borgne P, Koll F, Patel M, Dixon M, et al. C11orf70 mutations disrupting the intraflagellar transport-dependent assembly of multiple axonemal dyneins cause primary ciliary dyskinesia. Am J Hum Genet. 2018;102(5):956–72.
15. Coutton C, Martinez G, Kherraf ZE, Amiri-Yekta A, Boguenet M, Saut A, et al. Bi-allelic mutations in ARMC2 lead to severe astheno-teratozoospermia due to sperm flagellum malformations in humans and mice. Am J Hum Genet. 2019;104(2):331–40.
16. Soler Artigas M, Loth DW, Wain LV, Gharib SA, Obeidat M, Tang W, et al. Genome-wide association and large-scale follow up identifies 16 new loci influencing lung function. Nat Genet. 2011;43(11):1082–90.
17. Pereira GL, Malheiros JM, Ospina AMT, Chardulo LAL, Curi RA. Exome sequencing in genomic regions related to racing performance of Quarter Horses. J Appl Genet. 2019;60(1):79–86.
18. Björndahl L, Kirkman Brown J. The sixth edition of the WHO laboratory manual for the examination and processing of Human Semen: ensuring quality and standardization in basic examination of human ejaculates. Fertil Steril. 2022;117(2):246–51.
19. Li H, Durbin R. Fast and accurate short read alignment with Burrows-Wheeler transform. Bioinformatics. 2009;25(14):1754–60.
20. Wang K, Li M, Hakonarson H. ANNOVAR: functional annotation of genetic variants from high-throughput sequencing data. Nucleic Acids Res. 2010;38(16): e164.
21. Teves ME, Nagarkatti-Gude DR, Zhang Z, Strauss JF 3rd. Mammalian axoneme central pair complex proteins: Broader roles revealed by gene knockout phenotypes. Cytoskeleton (Hoboken). 2016;73(1):3–22.
22. Tewari R, Bailes E, Bunting KA, Coates JC. Armadillo-repeat protein functions: questions for little creatures. Trends Cell Biol. 2010;20(8):470–81.
23. Latour BL, Van De Weghe JC, Rusterholz TD, Letteboer SJ, Gomez A, Shaheen R, et al. Dysfunction of the ciliary ARMC9/TOGARAM1 protein module causes Joubert syndrome. J Clin Invest. 2020;130(8):4423–39.
24. Lu C, Zhang Y, Qin Y, Xu Q, Zhou R, Cui Y, et al. Human X chromosome exome sequencing identifies BCORL1 as contributor to spermatogenesis. J Med Genet. 2021;58(1):56–65.
25. Shimada K, Park S, Miyata H, Yu Z, Morohoshi A, Oura S, et al. ARMC12 regulates spatiotemporal mitochondrial dynamics during spermiogenesis and is required for male fertility. Proc Natl Acad Sci U S A. 2021;118(6):e2018355118.
26. Imtiaz F, Allam R, Ramzan K, Al-Sayed M. Variation in DNAH1 may contribute to primary ciliary dyskinesia. BMC Med Genet. 2015;16:14.
27. Neesen J, Kirschner R, Ochs M, Schmiedl A, Habermann B, Mueller C, et al. Disruption of an inner arm dynein heavy chain gene results in asthenozoospermia and reduced ciliary beat frequency. Hum Mol Genet. 2001;10(11):1117–28.
28. Guo T, Tu CF, Yang DH, Ding SZ, Lei C, Wang RC, et al. Bi-allelic BRWD1 variants cause male infertility with asthenoteratozoospermia and likely primary ciliary dyskinesia. Hum Genet. 2021;140(5):761–73.
29. Ge H, Zhou W, He M, Zheng H, Zhao X, Zhang T, et al. Mutations in CFAP47, a previously reported MMAF causative gene, also contribute to the respiratory defects in patients with PCD. Mol Genet Genomic Med. 2024;12(1):e2278.
30. Palermo G, Joris H, Devroey P, Van Steirteghem AC. Pregnancies after intracytoplasmic injection of single spermatozoon into an oocyte. Lancet. 1992;340(8810):17–8.
31. Chemes HE, Alvarez SC. Tales of the tail and sperm head aches: changing concepts on the prognostic significance of sperm pathologies affecting the head, neck and tail. Asian J Androl. 2012;14(1):14–23.

Publisher's Note